

EFFECTS OF NON-IDEAL ADSORPTION EQUILIBRIA OF GAS MIXTURES ON COLUMN DYNAMICS

Jeong-Ho Yun[†], Dae-Ki Choi, Sung-Hyun Kim* and Hee Moon**

Div. of Environment & CFC Technology, Korea Institute of Science & Technology,
P.O.Box 131, Cheongryang, Seoul 130-650, Korea

*Dept. of Chemical Engineering, Korea University, Seoul 136-701, Korea

**Dept. of Chemical Technology, Chonnam National University, Kwangju 500-757, Korea

(Received 19 May 1997 • accepted 15 July 1997)

Abstract – A theoretical study has been made for simulating the dynamic behavior of non-ideal gas mixtures in an isothermal fixed-bed adsorber. A mathematical model was developed which takes into account the non-ideality of adsorbable species on the adsorbed phase under equilibrium. The model is based on both the real adsorbed solution theory (RAST), which incorporates the activity coefficients in the multicomponent isotherm equations to account for the deviations from ideality, and the linear driving force (LDF) model for representing diffusion resistance inside the adsorbent particles. To describe the effect of non-ideal adsorption equilibrium of gas mixtures on the breakthrough curves, we considered several model mixtures of binary and ternary components which exhibit non-ideal behavior with azeotropic crossovers in the composition domains at equilibrium. Sample calculations of a fixed-bed adsorption were done with various inlet gas compositions of binary and ternary mixtures, respectively, at a fixed total concentration. From the calculation results, it was shown that the order of breakthrough curves could be changed at a certain value of inlet gas composition ratio. This result implies that the dynamic behaviors of fixed-bed adsorption are greatly influenced by multicomponent equilibrium models. Furthermore, the reversal phenomenon of breakthrough curves could not be simulated by the ideal adsorbed solution theory (IAST).

Key words: Fixed-bed Adsorption, Dynamic Behavior, Non-ideal Adsorption Equilibrium, Multicomponent System, Adsorbed Solution Theory

INTRODUCTION

When dealing with a multicomponent adsorption system, the performance of a fixed-bed column is defined by effluent concentration histories of various adsorbates present in the influent. Even for cases in which one need not to know the effluent concentration histories completely (in other words, only the information of certain species are needed), because of the interactions between the adsorbates, it is necessary to obtain them all. In general, for a multicomponent adsorption system, the interactions between the adsorbates can be classified into two kinds: one is the interaction between the adsorbates in their mass transfer, and the other is the interaction of the adsorbates in their distribution between the bulk and adsorbed phases at equilibrium. However, multicomponent mass transfer is a relatively unexplored field, and there exists little data that can be used for predicting the effect of interaction in mass transfer. Thus, in many cases, researchers working in the adsorption area ignore the effect due to this kind of interaction in adsorption calculations [Tien, 1994].

In general, the performance and operation cost of an adsorptive separation process depend upon the effectiveness of the process design and the efficiency of the process operation. Thus, rigorous approaches to the design and operation of adsorption systems must be considered to ensure efficient and

cost effective applications [Rota et al., 1993; Yun et al., 1996]. The reliable estimation of multicomponent equilibria is one of the key problems in the design of adsorptive separation units. For many decades, many efforts have been devoted to develop the adsorption theories for predicting multicomponent adsorption equilibria [Ruthven, 1984; Yang, 1987]. One of the most widely used models is the ideal adsorbed solution theory (IAST), developed by Myers and Prausnitz [1965]. This can easily be extended to non-ideal adsorbed solutions by introducing suitable activity coefficients for the adsorbed phase, leading to the real adsorbed solution theory (RAST). In many adsorption studies, IAST gives good predictions of multicomponent adsorption equilibrium. However, as noted by Gamba et al. [1990], when strongly adsorbable species are involved, the high surface coverage can induce deviations from ideality in the adsorbed phase.

In a recent study [Takeuchi et al., 1995], an interesting result was reported that the order of breakthrough curves could be changed according to influent gas compositions of binary mixtures, and it is believed that this phenomenon probably arises from either the non-ideality of the adsorbed phase or the effect of surface heterogeneity of an adsorbent. Owing to mathematical or computational complications, little attention has been given in studying these unusual adsorption behaviors in fixed-bed.

In this paper, an adsorption model is presented to simulate the multicomponent breakthrough curves from the isothermal

[†]To whom all correspondence should be addressed.

fixed-bed adsorption column, which is governed by non-ideal adsorption equilibrium. The model is based on both the real adsorbed solution theory (RAST), which incorporates the activity coefficients in the multicomponent isotherm equations to account for the deviations from ideality, and the linear driving force (LDF) model for representing diffusion resistance to mass transfer.

MODEL FORMULATION AND EQUILIBRIUM THEORY

A mathematical model was developed which takes into account the non-ideality of adsorbable species in the adsorbed phase under equilibrium. Applying the typical assumptions [Hwang, 1994] to the mass balance of the gas phase through a packed bed, the following governing equation for isothermal fixed-bed adsorption with N adsorbates was obtained:

$$\frac{\partial c_i}{\partial t} = D_L \frac{\partial^2 c_i}{\partial z^2} - v \frac{\partial c_i}{\partial z} - \frac{1-\varepsilon}{\varepsilon} \rho_p \frac{\partial n_i}{\partial t} \quad (1)$$

In Eq. (1), the mass transfer rate of the gas and the solid phase can be expressed as the following linear driving force (LDF) model for surface diffusion [Tien, 1994]:

$$\frac{\partial n_i}{\partial t} = k_s (n_i^* - n_i) = \frac{3k_f}{r_p \rho_p} (c_i - c_i^*) \quad (2)$$

where

$$k_s = \frac{15D_s}{r_p^2} \quad (3)$$

As denoted by Eqs. (2) and (3), the LDF model is an approximation to the solution of Fickian diffusion inside a spherical particle. This expression assumes that the mass transfer rate of adsorption is proportional to the difference between the equilibrium concentration and the bulk concentration of the component. Since the solution of the LDF model is much easier and faster than the solution of a diffusion model, we employed this model in the present study.

By introducing appropriate dimensionless variables, Eq. (1) can be written as follows:

$$\frac{\partial Y_i}{\partial \tau} = \frac{1}{Pe} \frac{\partial^2 Y_i}{\partial S^2} - \frac{\partial Y_i}{\partial S} + \alpha_i (Y_i - Y_i^*) \quad (4)$$

and the dimensionless variables are defined as follows:

$$Y_i = \frac{c_i}{c_{i0}}, \quad \tau = \frac{vt}{L}, \quad S = \frac{z}{L}, \quad Pe = \frac{vL}{D_L}, \quad \alpha_i = \frac{3k_f L}{r_p v} \left(\frac{1-\varepsilon}{\varepsilon} \right) \quad (5)$$

The associated initial condition for $0 < z < L$ is:

$$Y_i(z, 0) = 0 \quad (6)$$

and the boundary conditions at $z=0$ and $z=L$ for $t > 0$ are:

$$\frac{1}{Pe} \frac{\partial Y_i}{\partial S} \Big|_{z=0} = -(Y_i|_{z=0} - Y_i|_{z=0}) \quad (7)$$

$$\frac{\partial Y_i}{\partial S} \Big|_{z=L} = 0 \quad (8)$$

As previous researchers [Moon and Tien, 1987; Tien, 1994; Wang and Tien, 1982] pointed out in their works on fixed-bed adsorption, if the intraparticle diffusion is described by a homogeneous diffusion model or a lumped parameter model (such as the LDF model), one needs to calculate the concentrations in both phases at the same time. From Eq. (2), the following dynamic condition could be obtained:

$$c_i^* + A_i n_i^* = B_i \quad (9)$$

where

$$A_i = \frac{r_p \rho_p k_s}{3k_f} \quad \text{and} \quad B_i = c_i + A_i n_i \quad (10)$$

In order to calculate multicomponent breakthrough curves, the multicomponent adsorption isotherm should be incorporated into the mass balance equation of the fixed-bed adsorption column. For the multicomponent adsorption isotherm, we employed the adsorbed solution theory (AST) which was developed by Myers and Prausnitz [1965]:

$$c_i = c_T \gamma_i = \gamma_i(\vec{x}) x_i c_i^*(\pi) \quad (\text{constant } T) \quad (11)$$

where $c_i^*(\pi)$ is the standard state gas concentration (or pressure), which can be determined from the pure component adsorption isotherm, and $\gamma_i(\vec{x})$ is the activity coefficient of adsorbable species in the adsorbed phase. In the case of the ideal solution, the activity coefficients are equal to unity.

From the Gibbs' isotherm, the modified spreading pressure is given by:

$$\Pi = \frac{\pi A}{RT} = \int_0^{c_i^*} n_i^*(c_i^*) d \ln c_i^* \quad (12)$$

In the equilibrium state, the amount adsorbed, n_i^* , can be considered as:

$$n_i^* = n_T x_i \quad (13)$$

where n_T is total amount of adsorbed.

From Eqs. (9), (11) and (13), the useful relationships are obtained as follows:

$$x_i = \frac{B_i}{\gamma_i(\vec{x}) c_i^*(\pi) + A_i n_T} \quad (14)$$

$$n_T = \left(\sum_{i=1}^N \frac{x_i}{n_i^*} \right)^{-1} \quad (15)$$

and, also the following stoichiometric constraint should be considered:

$$\sum_{i=1}^N x_i = 1 \quad (16)$$

Using Eqs. (14), (16) and the given dynamic conditions, by Eq. (10), a set of N nonlinear equations is obtained:

$$\frac{B_1}{\gamma_1(\vec{x}) c_1^*(\pi) + A_1 n_T} - x_1 = 0$$

$$\frac{B_2}{\gamma_2(\vec{x}) c_2^*(\pi) + A_2 n_T} - x_2 = 0$$

$$\vdots$$

$$\frac{B_{N-1}}{\gamma_{N-1}(\bar{x})c_{N-1}^*(\pi) + A_{N-1}n_T} - x_{N-1} = 0$$

$$\sum_{i=1}^N \left(\frac{B_i}{\gamma_i(\bar{x})c_i^*(\pi) + A_i n_T} \right) - 1 = 0 \quad (17)$$

This set of nonlinear equations can be solved simultaneously for x_1 - x_{N-1} and π , using Newton's method [Yun et al., 1996].

To calculate the activity coefficients of each species, we employ the Wilson equation:

$$\ln \gamma_k = 1 - \ln \left[\sum_{j=1}^N x_j \Lambda_{kj} \right] - \sum_{j=1}^N \frac{x_j \Lambda_{jk}}{\sum_{j=1}^N x_j \Lambda_{ij}} \quad (18)$$

where Λ_{ij} is the interaction parameter between species i and j .

The system of model equations to be solved consists of the governing equation and the mass transfer equation (LDF model) as well as the multicomponent equilibrium model (AST). The partial differential equations (PDEs) representing the dynamics of the fixed-bed system are solved numerically. The PDEs are first reduced to a set of ordinary differential equations (ODEs) by the method of lines (MOL), and the resultant ODEs are integrated by LSODE as an integrator. LSODE employs Gear's stiff method with variable order and step size.

PREPARATION FOR MODEL SIMULATIONS

In the last section we used the RAST model to account for the deviation from ideality. And, with the LDF model for representing diffusion resistance of mass transfer, we developed the isothermal fixed-bed adsorption model. For the theoretical investigation of the breakthrough characteristics when the multicomponent system follows a non-ideal adsorption equilibrium, we consider the model mixtures of binary and ternary components. In most previous works dealing with the non-ideal adsorption, only negative deviations from Raoult's law have been reported for the adsorption of mixtures on microporous solids such as activated carbons, silica gel and H-mordenite [Minka and Myers, 1973; Peisen and Tiren, 1979; Costa et al., 1981; Talu and Zwiebel, 1986]. In this study, however, we also include the case of positive deviation from ideality.

The model mixtures are composed of three kinds of components, which will be denoted by comp. (1), comp. (2) and comp. (3). The Freundlich equation was chosen for representing the pure component equilibrium relationships, and the isotherm parameters of each species are listed in Table 1. These values were collected from experimental data of solvent vapors on activated carbon at 308 K [Kim, 1995].

$$\text{Freundlich equation: } n_i = K_i c_i^{1/m_i} \quad (19)$$

In order to introduce the non-ideality of each binary mix-

Table 1. Freundlich isotherm parameters of model species

	Comp. (1)	Comp. (2)	Comp. (3)
K	4.648	3.198	5.507
m	4.303	5.310	5.921

Table 2. The binary interaction parameters for using the Wilson equation

Deviations	Binary systems	Binary interaction parameters	
		Λ_{12}	Λ_{21}
Negative	comp. (1)-comp. (2)	3.028	9.065
	comp. (1)-comp. (3)	2.675	0.976
	comp. (2)-comp. (3)	11.08	4.949
Positive	comp. (1)-comp. (2)	0.194	0.392
	comp. (1)-comp. (3)	0.675	0.976
	comp. (2)-comp. (3)	0.556	0.729

ture of the adsorbed phase under equilibrium, we used the Wilson equation, with binary interaction parameters as given in Table 2. For the case of negative deviation, these values were collected from experimental binary data in the literature [Talu and Zwiebel, 1986], and for positive deviation, the values were also collected from experimental vapor-liquid equilibrium data [Prausnitz et al., 1986]. For the case of negative deviation, for example, the activity coefficients calculated using the Wilson equation, Eq. (18), are illustrated in Fig. 1, at a constant total concentration of 1.5 mol/m³ for comp. (1)-comp. (2) mixtures. The input parameters (e.g. adsorption bed and packing characteristics, kinetic parameters and adsorption conditions) used for model simulations are summarized in Table 3.

SIMULATION RESULTS

To investigate the effect of non-ideal adsorption equilibrium of gas mixtures on the dynamic behavior of a fixed-bed adsorption, the following cases were considered:

- (1) Binary mixtures of comp. (1)-comp. (2) with negative deviation.
- (2) Binary mixtures of comp. (1)-comp. (2) with positive

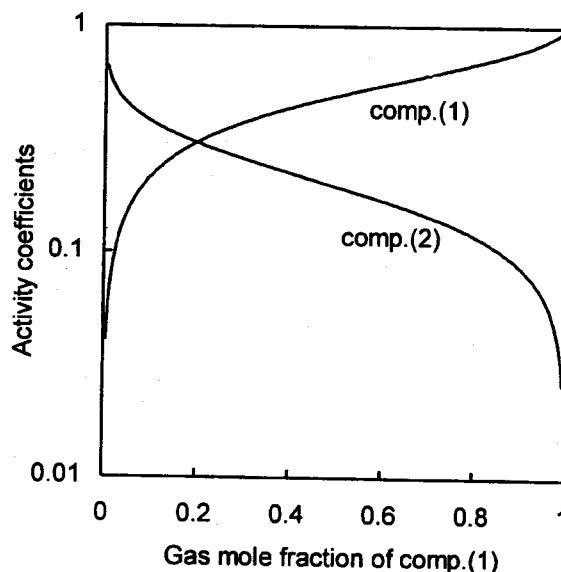


Fig. 1. Negative deviation of model binary mixture of comp. (1)-comp. (2).

[Wilson parameters are: $\Lambda_{12}=3.028$, $\Lambda_{21}=9.065$].

Table 3. Input parameters used for model simulations

Category	Parameter	Unit	Value
Bed and packing characteristics	Bed void fraction, ϵ	-	0.4
	Bed length, L	m	0.1
	Particle radius, r_p	m	1.7×10^{-3}
	Particle density, ρ_p	kg/m ³	800
Kinetic parameters	Axial dispersion coeff., D_L	m/s	1.0×10^{-6}
	film mass transfer coeff., k_f	m/s	3.5×10^{-3} (same for all)
	Surface diffusion coeff., D_{st}	m ² /s	9.0×10^{-10} (same for all)
Adsorption conditions	Fixed total concentration, c_T	mol/m ³	1.5
	Interstitial velocity, v	m/s	4.0×10^{-3}

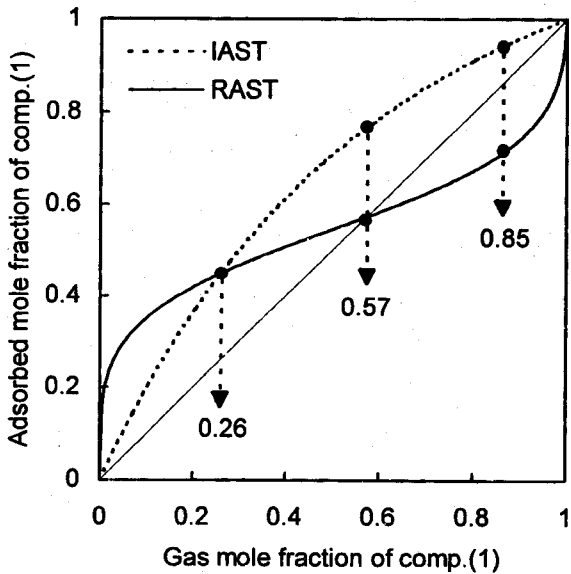


Fig. 2. Prediction of adsorbed mole fraction of model binary mixture of comp. (1)-comp. (2), for negative deviation. [$c_T=1.5 \text{ mol/m}^3$].

deviation.

(3) Ternary mixtures of comp. (1)-comp. (2)-comp. (3), when all binary mixtures exhibit negative deviations.

(4) Ternary mixtures of comp. (1)-comp. (2)-comp. (3), when all binary mixtures exhibit positive deviations.

For all cases, we first calculated the equilibrium relations at a constant total concentration of 1.5 mol/m^3 , and then it was compared with the results of the fixed-bed calculation.

For case (1), when the binary system exhibits a negative deviation from ideality, the calculated adsorbed phase mole fraction of comp. (1), using both the IAST and RAST models, are illustrated in Fig. 2, at a constant total concentration of 1.5 mol/m^3 . As shown in Fig. 2, when the RAST is applied to the equilibrium calculation, the model binary system of comp. (1) and comp. (2) exhibits the non-ideality with an azeotropic crossover in the composition domain. When the gas phase mole fraction of comp. (1) is 0.26, the calculated equilibrium mole fraction of the adsorbed phase is the same for the IAST and RAST models. And, when the gas phase mole fraction of comp. (1) is 0.57, quite different values of

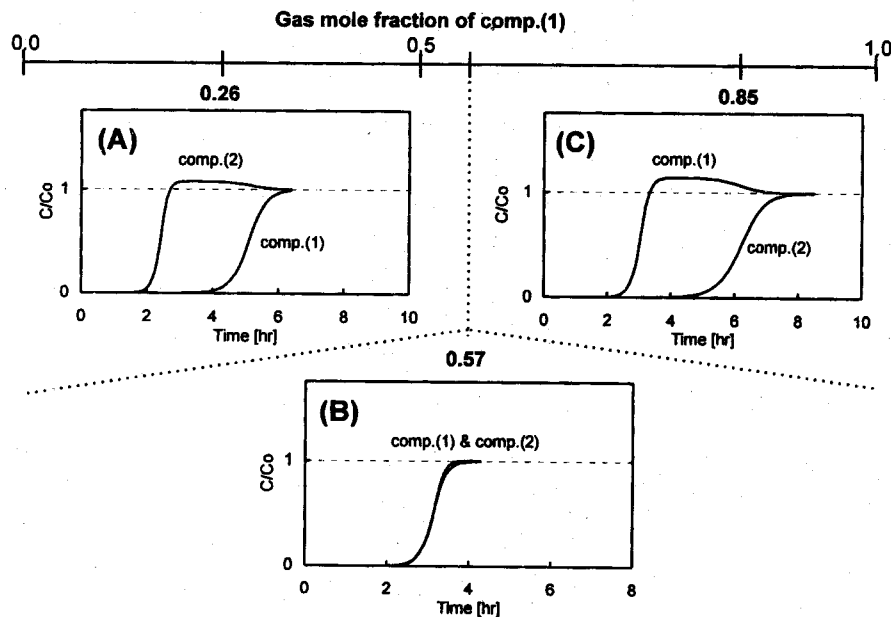


Fig. 3. Calculated breakthrough curves for model binary mixture of comp. (1)-comp. (2), for negative deviation. [$c_T=1.5 \text{ mol/m}^3$].

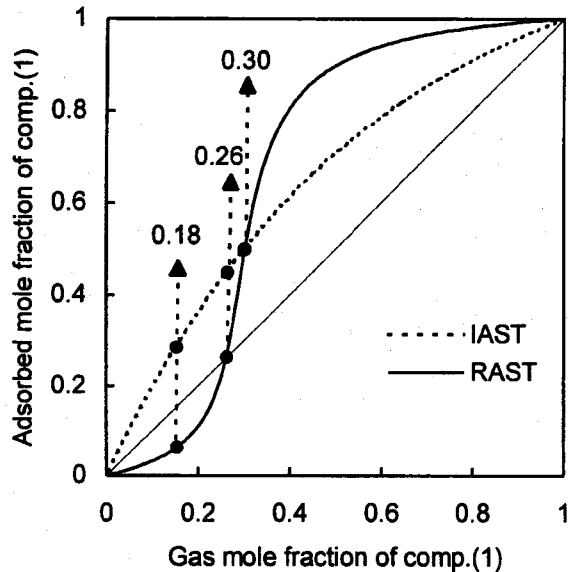


Fig. 4. Prediction of adsorbed mole fraction of model binary mixture of comp. (1)-comp. (2), for positive deviation. [$c_s=1.5 \text{ mol/m}^3$].

the adsorbed phase mole fractions are obtained from each equilibrium model. Also, the RAST model exhibits an azeotrope at this location. When the gas mole fraction of comp. (1) is 0.86, the calculated equilibrium mole fraction of the adsorbed phase for the IAST and RAST models are located on opposite sides of the diagonal. Using the mathematical model which was presented in the above section, several calculations of the fixed-bed adsorption were carried out at three equilibrium points (i.e. gas mole fractions of comp. (1) are: 0.26, 0.57 and 0.86). Simulation results are presented in Fig.

3, using the style of illustration proposed by Takeuchi et al. [1995]. As shown in Fig. 3, the calculated breakthrough curves were changed by the influent gas mole fraction. When the influent gas mole fraction of comp. (1) was less than 0.57, the breakthrough of comp. (2) took place earlier than that of comp. (1), as shown in Fig. 3(A). However, at the calculation point of 0.57, both comp. (1) and comp. (2) behave as if a single component, as shown in Fig. 3(B), and it should be noted that this azeotropic location (gas mole fraction of comp. (1) is 0.57) is same for the results of the equilibrium calculation using the RAST model. However, when the mole fraction was greater than 0.57, as shown in Fig. 3(C), the breakthrough of comp. (1) took place earlier than that of comp. (2) which showed the breakthrough order was reversed completely. These calculation results were qualitatively consistent with the experimental results of Takeuchi et al. [1995], and these unusual dynamic behaviors could not be simulated by any ideal equilibrium model, such as IAST.

For case (2), when the binary mixture exhibits a positive deviation from ideality, we also calculate the adsorbed phase mole fraction of comp. (1) at equilibrium, using both the IAST and RAST models. The calculation results are presented in Fig. 4. Similarly, three calculation points were considered, and its values are 0.18, 0.26 and 0.30, respectively. Also for the positive deviation, the reversal of breakthrough curves was observed by model simulations, and the results are presented in Fig. 5. When the influent gas mole fraction of comp. (1) was 0.18, the breakthrough of comp. (1) took place earlier than that of comp. (2), as shown in Fig. 5(A). However, both comp. (1) and comp. (2) are not separated clearly from each other. At the calculation point of 0.26, both comp. (1) and comp. (2) behave as if a single component, as shown in Fig. 5(B). It also should be noted that the location (0.26) is

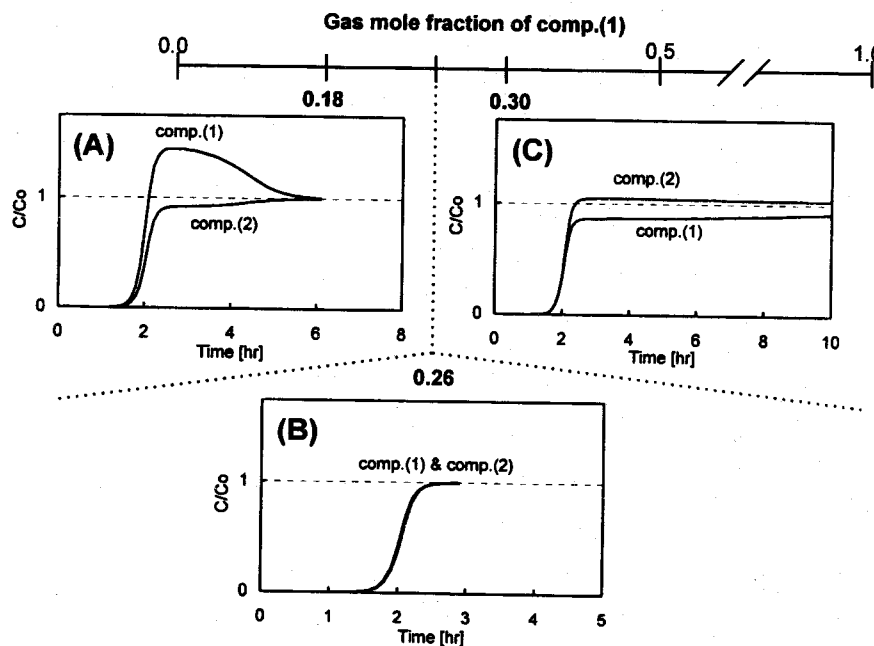


Fig. 5. Calculated breakthrough curves for model binary mixture of comp. (1)-comp. (2), for positive deviation. [$c_s=1.5 \text{ mol/m}^3$].

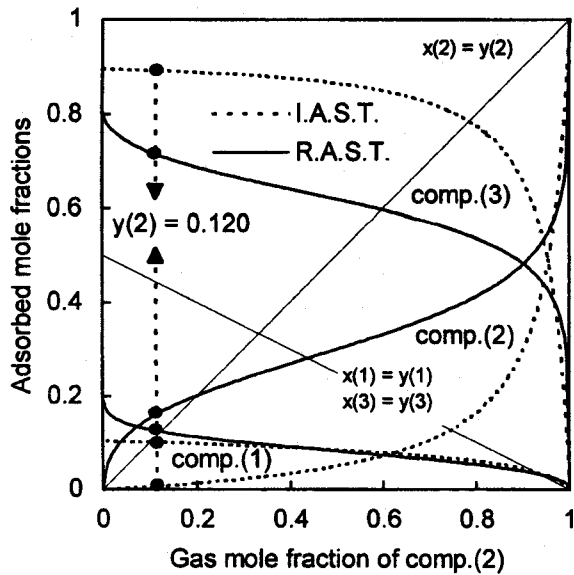


Fig. 6. Prediction of adsorbed mole fraction of model ternary mixture of comp. (1)-comp. (2)-comp. (3), for negative deviation.

$[c_T=1.5 \text{ mol/m}^3, y(1)/y(3)=1.0]$.

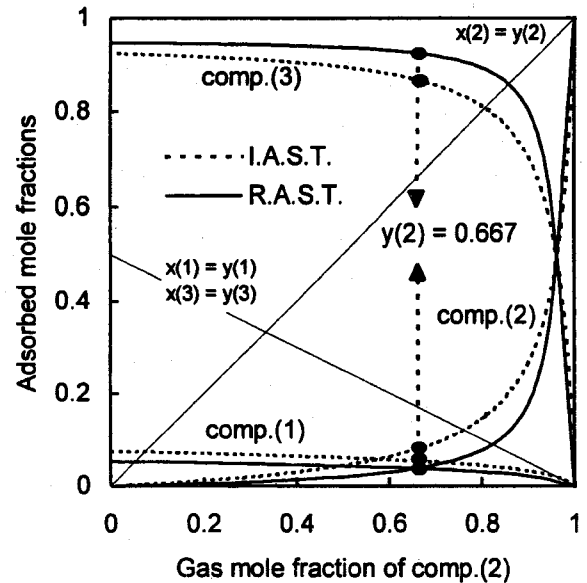


Fig. 8. Prediction of adsorbed mole fraction of model ternary mixture of comp. (1)-comp. (2)-comp. (3), for positive deviation.

$[c_T=1.5 \text{ mol/m}^3, y(1)/y(3)=0.665]$.

the same for the results of equilibrium calculation using the RAST model. When the mole fraction was greater than 0.26, as shown in Fig. 5(C), the breakthrough of comp. (2) took place earlier than that of comp. (1). In this case, however, the saturation time is too long, and the separation would practically be impossible.

For the ternary system when all binary mixtures exhibit negative deviations, case (3), the adsorbed phase mole frac-

tions of each species were calculated using both the IAST and RAST models, along the composition path of comp. (2). The calculation results are shown in Fig. 6. Model simulation was carried out at the equilibrium point of comp. (2) is 0.12 (comp. (1) and comp. (3) are both 0.44). From these equilibrium conditions, the breakthrough curves of the model ternary mixture were calculated. The calculation results are presented in Fig. 7. As shown in Fig. 7, we compared the cal-

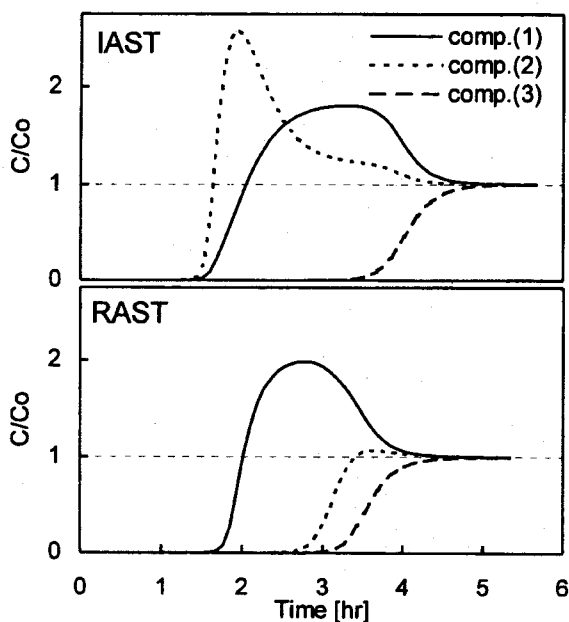


Fig. 7. Calculated breakthrough curves for model ternary mixture of comp. (1)-comp. (2)-comp. (3), for negative deviation.

$[c_T=1.5 \text{ mol/m}^3, y(2)=0.12, y(1)/y(3)=1.0]$.

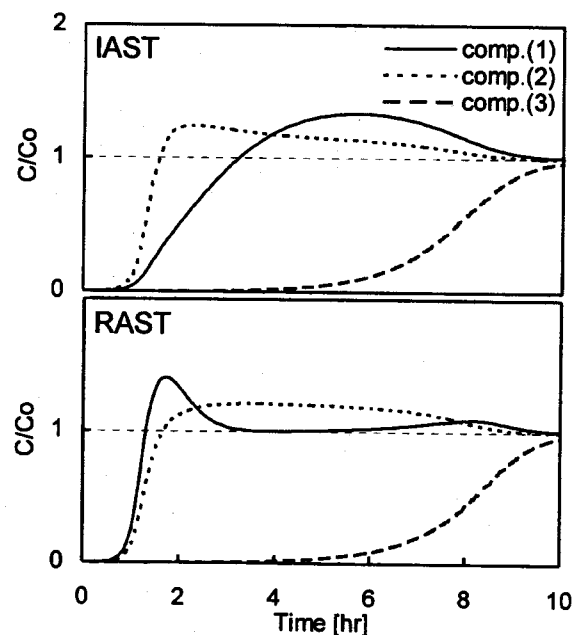


Fig. 9. Calculated breakthrough curves for model ternary mixture of comp. (1)-comp. (2)-comp. (3), for positive deviation.

$[c_T=1.5 \text{ mol/m}^3, y(2)=0.667, y(1)/y(3)=0.665]$.

ulation results for each equilibrium model. When the IAST model was employed, the breakthrough of comp. (2) took place earlier than that of comp. (1). In this case, comp. (3) is completely separated from both comp. (1) and comp. (2). However, the simulation results using the RAST model, showed that comp. (1) is completely separated from both comp. (2) and comp. (3). However, each species of comp. (2) and comp. (3) cannot be separated from each other.

Finally, for the ternary system when all the binary mixtures exhibit positive deviations, case (4), the adsorbed phase mole fractions of each species were also calculated using both models, along the composition path of comp. (2). The calculation results are shown in Fig. 8. As can be seen, the equilibrium mole fractions of comp. (1) and comp. (2) were nearly overlapped at which the point of comp. (2) is 0.667 (comp. (1) and comp. (3) are 0.133 and 0.2, respectively), for both the IAST and RAST models. Thus, it can be expected that there will be a high competition of both comp. (1) and comp. (2) in the fixed-bed adsorption column. Model simulation was performed at this equilibrium condition, and the results are presented in Fig. 9. As mentioned above, the separation of comp. (1) and comp. (2) is practically impossible for both the IAST and RAST models. Especially, when the RAST model was employed, the severe competitions were observed between comp. (1) and comp. (2). Consequently, the breakthrough of these species were reversed twice at this equilibrium point.

CONCLUSIONS

In this study, a mathematical model was developed to simulate the multicomponent breakthrough curves for isothermal fixed-bed adsorption which is governed by a non-ideal adsorption equilibrium. The model is based on both the real adsorbed solution theory (RAST), which incorporates the activity coefficients in the multicomponent isotherm equations to account for the deviations from ideality, and the linear driving force (LDF) model for representing diffusion resistance inside the adsorbent particles. From model simulations, it was clearly proven that dynamic behaviors of a fixed-bed adsorption are greatly influenced by the multicomponent adsorption equilibrium models. Also, the reversal phenomenon of breakthrough curves cannot be simulated by an ideal equilibrium model, such as the ideal adsorbed solution theory (IAST).

ACKNOWLEDGEMENT

This study was supported by Korea Science and Engineering Foundation (No. 961-1107-043-2).

NOMENCLATURE

- A : specific area of adsorbent [m^2]
 A_i : dynamic condition of component i
 B_i : dynamic condition of component i
 c_i : bulk phase concentration of component i [mol/m^3]
 $c_i^*(\pi)$: equilibrium concentration of component i corresponding to π [mol/m^3]
 c_o : influent gas concentration [mol/m^3]

- c_T : total concentration [mol/m^3]
 D_L : axial dispersion coefficient [m^2/s]
 D_{si} : surface diffusion coefficient [m^2/s]
 K_i : Freundlich equation parameter of component i
 k_{fi} : fluid film mass transfer coefficient of component i [m/s]
 k_{si} : LDF mass transfer coefficient of component i [$1/\text{s}$]
 L : bed length [m]
 m_i : Freundlich equation parameter of component i
 N : number of component
 n_i : amount adsorbed of component i at equilibrium [mol/kg]
 n_i^* : amount adsorbed of component i at pure state [mol/kg]
 n_T : total amount adsorbed [mol/kg]
 R : gas constant
 r_p : particle radius [m]
 S : dimensionless axial distance
 T : absolute temperature [K]
 t : time
 x_i : adsorbed phase mole fraction of component i
 Y_i : dimensionless concentration of component i
 y_i : gas phase mole fraction of component I
 z : axial distance coordinate [m]

Abbreviations

- AST : adsorbed solution theory
 comp.(i) : model component i
 IAST : ideal adsorbed solution theory
 LDF : linear driving force
 LSODE : livermore solver for ordinary differential equations
 MOL : method of lines
 ODE : ordinary differential equation
 PDE : partial differential equation
 Pe : Peclet number
 RAST : real adsorbed solution theory

Greek Letters

- α_i : dimensionless variable
 ϵ : bed void fraction
 γ_i : activity coefficient of component i
 Λ_{ij} : interaction parameter of Wilson equation
 v : interstitial velocity [m/s]
 Π : modified spreading pressure
 π : spreading pressure
 ρ_p : Particle density [kg/m^3]
 τ : dimensionless time

REFERENCES

- Costa, E. J. L., Sotelo, J. L., Calleja, G. and Marron, C., "Adsorption of Binary and Ternary Hydrocarbon Gas Mixtures on Activated Carbon: Experimental Determination and Theoretical Prediction of the Ternary Equilibrium Data", *AIChE J.*, **27**, 5 (1981).
 Gamba, G., Rota, R., Carra, S. and Morbidelli, M., "Adsorption Equilibria of Nonideal Multicomponent Systems at Saturation", *AIChE J.*, **36**, 1736 (1990).
 Hwang, K. S., "Separation of H_2/CO_2 , H_2/CO Gas Mixtures by Pressure Swing Adsorption and Fixed-Bed Dynamics", Ph.D dissertation, KAIST (1994).

- Kim, D. J., M. S. Thesis, Chonnam National University (1995).
- Minka, C. and Myers, A. L., "Adsorption from Ternary Liquid Mixtures on Solids", *AIChE J.*, **19**, 453 (1973).
- Moon, H. and Tien, C., "Further Work on Multicomponent Adsorption Equilibria Calculations Based on the Ideal Adsorbed Solution Theory", *Ind. Eng. Chem. Res.*, **26**, 2042 (1987).
- Myers, A. L. and Prausnitz, J. M., "Thermodynamics of Mixed Gas Adsorption", *AIChE J.*, **11**, 121 (1965).
- Peisen, L. and Tiren, G., "Thermodynamics of Adsorption from Perfect Binary Liquid Mixtures on Silica Gel", *Scientia Sinica*, **22**, 1384 (1979).
- Prausnitz, J. M., Lichtenthaler, R. N. and Azevedo, E. G., "Molecular Thermodynamics of Fluid-Phase Equilibria", Prentice-Hall, New Jersey (1986).
- Rota, R., Gamba, G. and Morbidelli, M., "On the Use of the Adsorbed Solution Theory for Designing Adsorption Separation Units", *Sep. Technol.*, **3**, 230 (1993).
- Ruthven, D. M., "Principles of Adsorption and Adsorption Processes", John Wiley & Sons (1984).
- Takeuchi, Y., Iwamoto, H., Miyata, N., Asano, S. and Harada, M., "Adsorption of 1-Butanol and p-Xylene Vapor and Their Mixtures with High Silica Zeolites", *Sep. Technol.*, **5**, 23 (1995).
- Talu, O. and Zwiebel, I., "Multicomponent Adsorption Equilibria of Nonideal Mixtures", *AIChE J.*, **32**, 1263 (1986).
- Tien, C., "Adsorption Calculations and Modeling", Butterworth-Heinemann (1994).
- Wang, S. C. and Tien, C., "Further Work on Multicomponent Liquid Phase Adsorption in Fixed Beds", *AIChE J.*, **28**, 565 (1982).
- Yang, R. T., "Gas Separation by Adsorption Processes", Butterworth, New York (1987).
- Yun, J. H., Park, H. C. and Moon, H., "Multicomponent Adsorption Calculations Based on Adsorbed Solution Theory", *KJChE*, **13**(3), 246 (1996).